DALTON
FULL PAPER

Crystal supramolecular motifs. Two- and three-dimensional networks of Ph_4P^+ cations engaged in sixfold phenyl embraces

Marcia Scudder and Ian Dance *

School of Chemistry, University of New South Wales, Sydney 2052, Australia.
E-mail: I.Dance@unsw.edu.au

Received 8th May 1998, Accepted 23rd July 1998

The sixfold phenyl embrace (6PE) which is a widespread supramolecular motif for Ph_4P^+ cations in crystals can occur as a zig-zag chain motif (ZZI6PE) in which each Ph_4P^+ engages two 6PE, and these ZZI6PE allow further multiple phenyl embraces at each Ph_4P^+ cation. The Cambridge Structural Database has been explored for occurrences of the two- and three-dimensional networks of multiple phenyl embraces involving the common cation Ph_4P^+. A prevalent motif involves parallel ZZI6PE chains linked by fourfold phenyl embraces (the parallel variant, P4PE) to form skewed hexagonal nets, called ZZI6PE/P4PE layers. Another type has ZZI6PE chains running in orthogonal directions and linked by the orthogonal variant of the 4PE: these are the orthogonal ZZI6PE/O4PE three-dimensional nets. An expanded layer involves eight-rings of Ph_4P^+ built from finite sequences of 6PE. The compounds $[Ph_4P^+]_2[Te_4]^{2-}$ and $[Ph_4P^+]_4[(S_6)Cu(S_8)Cu(S_6)]^{4-}$ contain more elaborate three-dimensional nets comprised of 6PE, 4PE and 3PEs. These nets are more highly concerted crystal supramolecular motifs. The nets described are different from those based on 4PE, and the difference is related to the charge of the anion. Anions are usually located over or in the cycles of cations in the layered motifs, and in cavities of the three-dimensional motifs. The concerted supramolecular motifs of cations, rather than cation–anion attractions, are believed to be the dominant factors in the crystal supramolecularity. Calculated energies for the motifs are reported. It is concluded that a single Ph_4P^+ cation can participate in up to four multiple phenyl embraces, and that the maximum attractive interaction energy per Ph_4P^+ cation is *ca.* 9 kcal mol^{-1}. This is comparable with the energies of hydrogen bonds.

Introduction

A feature of the supramolecularity of phenylated molecules is the widespread occurrence of multiple phenyl embraces, in which individual intermolecular phenyl···phenyl attractive interactions operate in concert with significant net attraction.[1–7] These supramolecular motifs have been recognised through analysis of the packing in molecular crystals (supramolecular entities par excellence[8,9]) using the voluminous accurate geometrical data in the Cambridge Structural Database.[10] The characteristic attributes of multiple phenyl embraces are (1) participation of two or more phenyl groups from each partner molecule, (2) geometrical concertedness, and (3) strong attraction. The most prevalent multiple phenyl embrace is the sixfold phenyl embrace, 6PE, in which three phenyl rings from each molecule are involved in six edge-to-face local phenyl···phenyl attractions: the net attractive energy of the 6PE is in the range 8–11 kcal mol^{-1}.† The other major type is the fourfold phenyl embrace, 4PE, which has orthogonal and parallel variants, namely the O4PE and P4PE respectively.

The 6PE, O4PE and P4PE motifs are illustrated in the preceding paper,[7] where we described how Ph_4P^+ cations in crystals can form one-, two- and three-dimensional networks constructed from 4PE. In this paper we describe two- and three-dimensional networks comprised of Ph_4P^+ cations linked mainly by 6PE. We have previously identified and described the one-dimensional ziz-zag infinite chain of sixfold phenyl embraces (ZZI6PE) involving Ph_4P^+. In the ZZI6PE, each 6PE uses three phenyl rings or one face of the Ph_4P^+ tetrahedron, and the two faces or 6PE are therefore inclined at the tetrahedral angle at the P atom, giving rise to the zig-zag.[11] In the ZZI6PE the required threefold array within each of the two sets of three phenyl rings for each 6PE is allowed by the intramolecular constraints on the conformations of the phenyl rings in Ph_4X.[12]

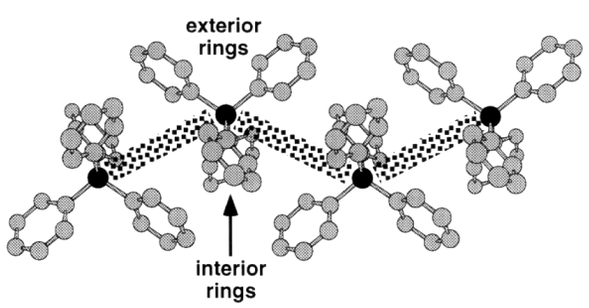

ZZI6PE

At each Ph_4P^+ in the ZZI6PE the two phenyl rings on the interior of the bend are engaged in the two 6PE, but each of the two phenyl rings on the exterior of the bend is engaged in only one 6PE, and is still available for involvement in further multiple phenyl embraces. It is these additional embraces which give rise to the networks described in this paper.

Methodology

The use of the Cambridge Structural Database, and the calculational procedures for evaluation of attractive energies, are described in the preceding paper.[7] van der Waals radii used in the calculations of volumes are Fe 2.0, S 1.8, Br 1.85, I 1.98 and H 1.1 Å. In the Fig. captions the calculated energies of specific multiple phenyl embraces (identified by their P···P distances) are quoted in kcal mol^{-1} per $\{Ph_4\}_2$ set, and [in

† These intermolecular energies are calculated as the sum of the van der Waals and coulombic atom–atom components, dependent on empirical parameters which are under continuing revision: more recent energy values may differ from earlier published values.

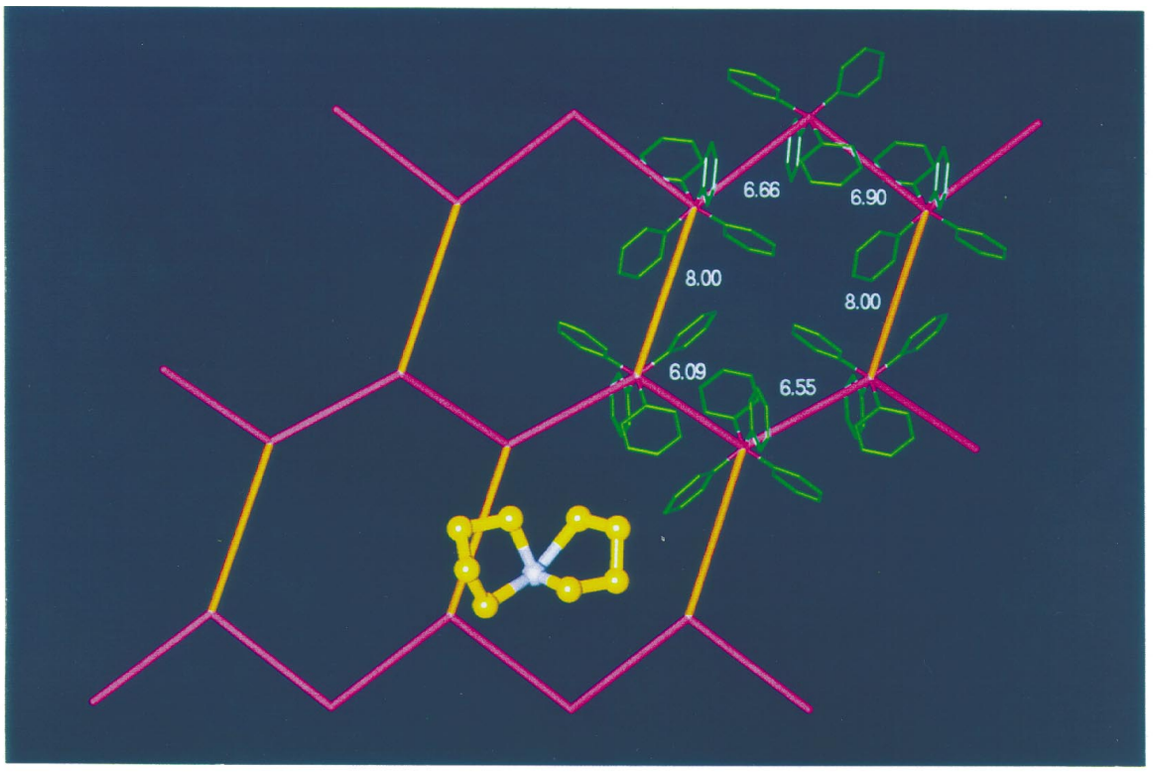

Fig. 1 Representation of the multiple phenyl embraces in crystalline $[Ph_4P^+]_2[Pb(Se_4)_2]^{2-}$ [VIPTAP]. The chains of 6PE are denoted by purple rods, and the P4PE motifs which connect them are shown as orange rods, with a minimal set of phenyl rings which comprise the interactions also drawn. There are two crystallographically distinct ZZI6PE chains, with 6PE interactions identified by their P···P distances of 6.09, 6.55 Å alternating in one chain and 6.66, 6.90 Å alternating in the other: all P4PE interactions have P···P 8.00 Å, and all P atoms lie in the same plane. One anion, located over the approximately hexagonal gap in the cation layer, is shown. The calculated energies of the embraces (identified by their P···P distances) are given in kcal mol^{-1} per $\{Ph_4\}_2$ set, and in square brackets per $\{Ph_4P\}_2$ set: 6PE at 6.09 Å, −10.4 [−7.4]; 6PE at 6.55 Å −6.8 [−3.8]; 6PE at 6.66 Å −8.0 [−4.6]; 6PE at 6.90 Å −5.8 [−2.7]; P4PE at 8.00 Å −5.9 [−2.8] kcal mol^{-1}.

square brackets] per $\{Ph_4P\}_2$ set. In Table 3 the energies are presented as net attractive energies between one Ph_4P^+ cation and its neighbouring Ph_4P^+ cations.

Results

The hexagonal ZZI6PE/P4PE layer

The two exterior phenyl rings just mentioned can readily form a P4PE, as is illustrated in Fig. 1, for the compound $[Ph_4P^+]_2[Pb(Se_4)_2]^{2-}$ [VIPTAP]. The ZZI6PE chains are denoted by purple rods, and the P4PE motifs which connect them are shown as orange rods. This motif, called the hexagonal ZZI6PE/P4PE layer, has an approximately planar net of P atoms. The characteristic of the parallel 4PE is that the C_{ipso}–P–C_{ipso} planes on the two molecules are exactly or almost coplanar (see previous paper[7]), and consequently the two phenyl rings at each P have inequivalent roles. Therefore the contiguous ZZI6PE chains in the ZZI6PE/P4PE layer do not exactly oppose each other, but are partly displaced along their length in order to optimise the geometry of the P4PE, as is evident in Fig. 1. This collection of cations forms a concerted two-dimensional motif, in which each cation is three-connected, and the array of cations is distorted hexagonal. The calculated attractive energies of the various interactions are provided in the caption to Fig. 1.

Table 1 lists the many other instances of this crystal packing type. One distinctive characteristic of crystals which adopt this hexagonal ZZI6PE/P4PE layer motif is their space group, which is almost invariably $P\bar{1}$. It is to be noted that the anions are generally small, and that the anionic metal complexes have monatomic or oligoatomic ligands. Almost all of the anions have double negative charge, with the consequence that one anion is associated with each distorted hexagon of cations, as in Fig. 1. In general (although not in VIPTAP, Fig. 1), the anion is situated at one of the inversion centres *between* the layers. Solvent molecules occupy lattice holes in a number of structures, and are related by another of the inversion centres. When the charge is single negative, there are two anions associated with each hexagon, related by one of the inversion centres: BUNHEX, COGHEL, PASWIP, BIHDAX, TAGFAI and JEDIAC01 fall into this category.

The predominance of space group $P\bar{1}$ is entirely in accord with, and a demonstration of, a principle of crystal packing enunciated by Brock and Dunitz.[13] They drew attention to the favourability of the centre of inversion as a symmetry element for intermolecular motifs, and the unfavourability of rotation axes and mirror planes as intermolecular symmetry elements. Both the 6PE and the P4PE can accommodate a centre of inversion without distortion: the 6PE requires heterochiral partners, and is disposed towards centrosymmetry. The space group which combines only centres of inversion and translation is $P\bar{1}$. Intramolecular symmetry possible for Ph_4P^+ is restricted to S_4 and subsets D_2 and C_2, but since these cannot be incorporated in the 6PE or P4PE motifs, the cation array can only support space group $P\bar{1}$. In most of the few examples in Table 1 with higher symmetry space groups, the anions are located on two-fold special positions, and the embraces populate the centres of inversion (except in the cases of FAZPEB and FOBNAL).

There are two examples in Table 1 which include mixed cations, JEGBAY and ZIPROF, both of which contain a similar pseudo-hexagonal array of multiply embracing Ph_4P^+ cations. In $[Ph_4P^+]_2$ $[Bu_4N^+]_2[Fe_8S_9Cl_6]^{4-}$ [JEGBAY] there is one anion associated with each pseudo-hexagon of cations. However, the anion is 4−, and the crystal also contains Bu_4N^+ cations equal in number to the Ph_4P^+ cations. As shown in Fig. 2 there is a clear segregation of the Bu_4N^+ cations from

Table 1 Crystal structures containing the hexagonal ZZI6PE/P4PE layer. All structures have space group $P\bar{1}$ unless otherwise stated. The listing groups compounds with chemically similar anions

Refcode	Anion	P···P distances in the ZZ16PE/Å	P···P distances in the P4PE/Å
CUTMEJ	$[Br_2Se(\mu\text{-}Br)_2SeBr_2]^{2-}$	6.51, 6.69	8.36
VIKJAA	$[Cl_2Se(\mu\text{-}Cl)_2SeCl_2]^{2-}$	6.34, 6.54	8.18
JAVYOU	$[Se_2W(\mu\text{-}Se)_2WSe_2]^{2-}$	6.47, 6.89	8.05
KAVHEU	$[Cl_2Zn(\mu\text{-}Cl)_2ZnCl_2]^{2-}$	6.52, 6.71	8.14
KAVHIY	$[Cl_2Cd(\mu\text{-}Cl)_2CdCl_2]^{2-}$	6.58, 6.63	8.25
GAYWIM	$[Br_2Mn(\mu\text{-}Br)_2MnBr_2]^{2-}$	6.59, 6.60	8.42
BIRHAL10	$[OCl_2Se(\mu\text{-}Cl)_2SeCl_2O]^{2-}$	6.45, 6.49	8.39
FUYXEC	$[WS_2Cl_4]^{2-}\cdot 2CH_2Cl_2$	6.37, 6.77	8.43
GAZNOK	$[RuCl_4]^{2-}\cdot 2CH_2Cl_2$	6.38, 6.78	8.42
GAZNUQ	$[UCl_6]^{2-}\cdot 2CH_2Cl_2$	6.42, 6.83	8.55
JAVKEW	$[ZrCl_6]^{2-}\cdot 2CH_2Cl_2$	6.41, 6.81	8.50
COYWES	$[WOCl_5]^{2-}\cdot 2CH_2Cl_2$	6.37, 6.76	8.37
COYWIW	$[ReOCl_5]^{2-}\cdot 2CH_2Cl_2$	6.34, 6.73	8.41
SIWKUE	$[NbSCl_5]^{2-}\cdot 2CH_2Cl_2$	6.37, 6.81	8.47
FUWSAR	$[Cl_4ReReCl_4]^{2-}\cdot 2CH_2Cl_2$	6.13, 6.61	8.45
TOSYIJ	$[NC\text{-}Se\text{-}B_6H_5]^{2-}$	6.15, 6.27	7.99
TOSYUV	$[NC\text{-}Se\text{-}B_{12}H_{11}]^{2-}\cdot CH_3CN$	6.08, 6.16	8.30
DEMYEZ01	Br^-	6.33, 6.40	7.92
VAXDUT	$Br^-\cdot H_2O$	6.31, 6.39	7.91
FAZPEB *C*2/*c*	$[S(S_2)_2W(\mu\text{-}S)W(S_2)_2S]^{2-}\cdot CH_3CN$	6.53, 6.53	8.73
FOBNAL *Pbcn*	$[O(S_2)_2W(\mu\text{-}S)W(S_2)_2O]^{2-}\cdot CH_3CN$	6.68, 6.68	8.98
BUNHEX	$[MoBr_3(NO)_2OH_2]^-$	6.51, 6.58	8.55
COGHEL	$[RuCl_4(NS)OH_2]^-$	6.70, 6.80	8.42
CEXRIG	$[OsCl_6]^{2-}\cdot DMF$	6.37, 6.58	8.57
VIPTAP	$[Pb(Se_4)_2]^{2-}$	6.09, 6.55	8.00
		6.66, 6.90	
KAZBUI10	$[Pt(Se_4)_3]^{2-}\cdot DMF$	6.26, 6.89	8.78
		6.26, 6.89	8.54
PERGIC	$[Tl_2(S_4)_2]^{2-}$	6.41, 6.44	8.88
YOLGEL	$[(CO)_4Mo(\mu\text{-}S)_2Mo(\mu\text{-}S)_2Mo(CO)_4]^{2-}$	6.45, 6.60	8.36
YOLGIP	$[(CO)_4W(\mu\text{-}S)_2W(\mu\text{-}S)_2W(CO)_4]^{2-}$	6.48, 6.70	8.32
ZAZBIL	$[Ag_2Se_6Te_3]^{2-}$	6.47, 6.66	8.13
VOFMOS	$[(\mu\text{-}Se_3)(\mu\text{-}Se_2)Au_2]^{2-}$	6.22, 6.29	7.96
		6.20, 6.29	
VOFNAF *C*2/*c*	$[(\mu\text{-}Se_4)(\mu\text{-}Se_2)Au_2]^{2-}$	6.44, 6.44	8.20
RARZEP	$[OV\{OP(O)(CH_3)OP(O)(CH_3)O\}_2]^{2-}$	6.28, 6.54	8.05
PASWIP	$[OAs(OH)_3]Cl^-$	6.27, 6.43	8.98
TAGFAI	$[CH_3C(=NH)Cl]Cl^-$	6.14, 6.62	8.11
WACXAZ	$[Hg(c\text{-}C_6H_8S_2)_2]^{2-}\cdot 4H_2O$	6.58, 6.65	8.41 skewed
		6.07, 6.58	P4PE
WACXED	$[Cd(c\text{-}C_6H_8S_2)_2]^{2-}\cdot 4H_2O$	6.62, 6.64	8.42 skewed
		6.06, 6.62	P4PE
DURXUJ *C*2/*c*	$[Pd(SCH_2CH_2S)_2]^{2-}\cdot 4H_2O$	6.12, 6.86	8.34
BIHDAX	$[Me_2SMoCl_2(\mu\text{-}Cl)_3MoCl_2SMe_2]^-$	6.32, 6.34	8.58
JEDIAC01 $P2_1/c$	$[SRe(S_4)_2]^-$	6.93, 6.93	8.79
POJRAH02 *Ccca*	$[\{Cu_3I_4\}^-]\infty$	6.42, 6.42	8.70
VECGUF10	$[OW(CN)_6]^{2-}\cdot H_2O$	6.56, 6.95	7.15
VOXWOU	$[Cl_2Sb(\mu\text{-}S)(\mu\text{-}Cl)_2SbCl_2]^{2-}\cdot CH_3CN$	6.31, 6.42	8.75
		6.42, 6.68	8.75
ZIPROF	$[Mo_6Se_2Cl_{12}]^{4-}[H_3O^+]_2\cdot 4CH_3OH$	6.47, 6.71	8.50
ZAQRUE01	$[SeSb_4(Se)_4Se]^{2-}$	6.05, 6.72	7.98
JEGBAY *C*2/*c*	$[(Cl_3Fe_4S_4)(\mu\text{-}S)(Fe_4S_4Cl_3)]^{4-}[Bu_4N^+]_2[Ph_4P^+]_2$	6.34, 6.88	8.86
JANHIP10[a]	$[(Se_4)_2InSe_5In(Se_4)_2]^{4-}$	6.43, 6.99	8.60
KOMWUE[b]	$[Cl_3W(\mu\text{-}SEt)(\mu\text{-}Cl)(\mu\text{-}SEt_2)WCl_3]^{2-}\cdot CH_2Cl_2$	6.34, 6.34	8.53
PAHPOD[c]	$[\{Cr(CO)_5\}_2TeTe\{Cr(CO)_5\}_2]^{2-}\cdot CH_2Cl_2$	6.39, 6.90	8.96

[a] Additional chains of alternating 6PE (6.22 Å) and P4PE (8.37 Å). [b] Additional layers composed of 6PE (5.73) and P4PE (7.97 and 8.10 Å). [c] Additional layers composed of 6PE (6.46) and P4PE (8.10 and 8.28 Å).

the Ph_4P^+ cations in the hexagonal ZZI6PE/P4PE array. This segregation is a manifestation of the dominance of the attractive energies in the two-dimensional network of multiple phenyl embraces.

The orthogonal ZZI6PE/O4PE net

In the ZZI6PE the two phenyl groups exterior to the chain at each cation are symmetrically arrayed in the plane of the chain. Two ZZI6PE chains orthogonal to each other could therefore form an O4PE between pairs of these orthogonal phenyl groups, and this motif indeed occurs, albeit usually distorted, in the crystal structures of the compounds listed in Table 2. A good example is $[Ph_4P^+]_2[Fe_4S_4(SH)_4]^{2-}$ [FAGREK], shown in Fig. 3. All except one of the compounds listed in Table 2 adopt space group *C*2/*c* where the equivalent ZZI6PE chains align with the *ab* diagonals of the unit cell. However, these structures are not as ideally orthogonal in the 4PE as hinted above because the two C_{ipso}–P–C_{ipso} planes are not orthogonal. Table 2 contains details of the angles between the normals to the two C_{ipso}–P–C_{ipso} planes involved in the 4PE: these values range from 38 to 68°, while in the ideal O4PE this angle is 90°. It is evident from Fig. 3 that this apparent distortion is mainly local.

The crystal structure of $[Ph_4P^+]_2[Fe_4S_4Br_4]^{2-}$ [DEXXIN10] is very similar to that of the related compound $[Ph_4P^+]_2$-

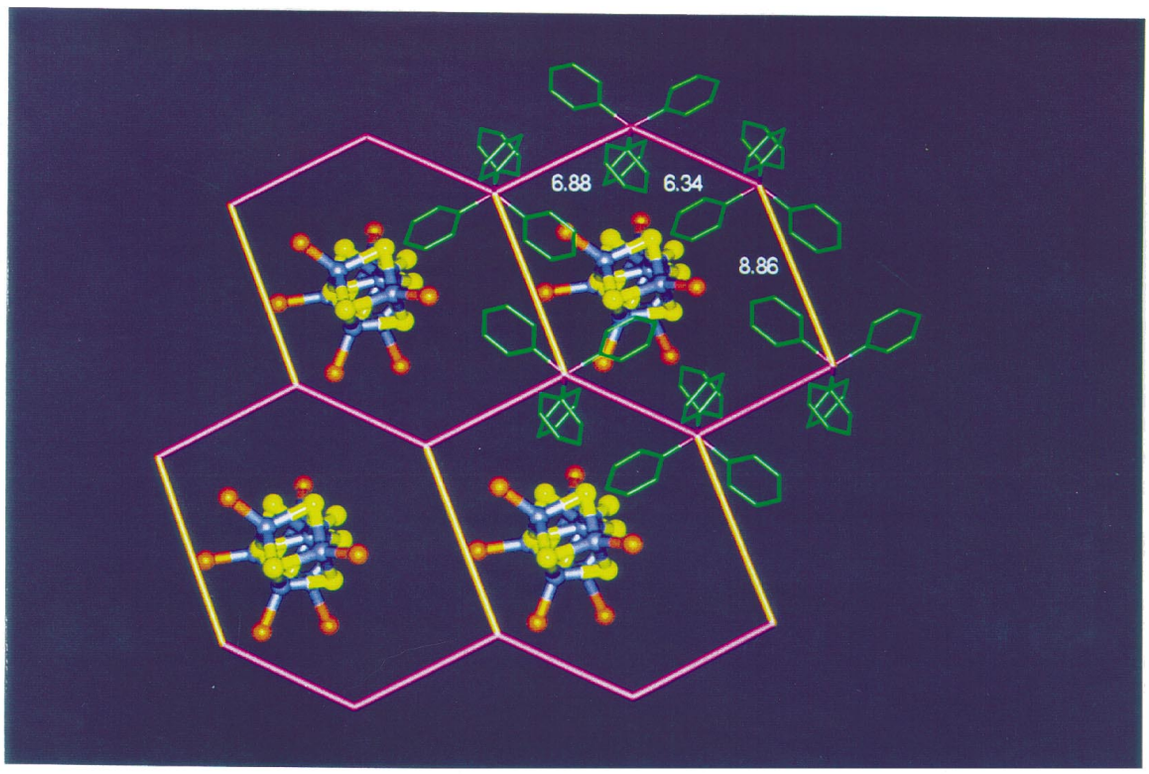

(a)

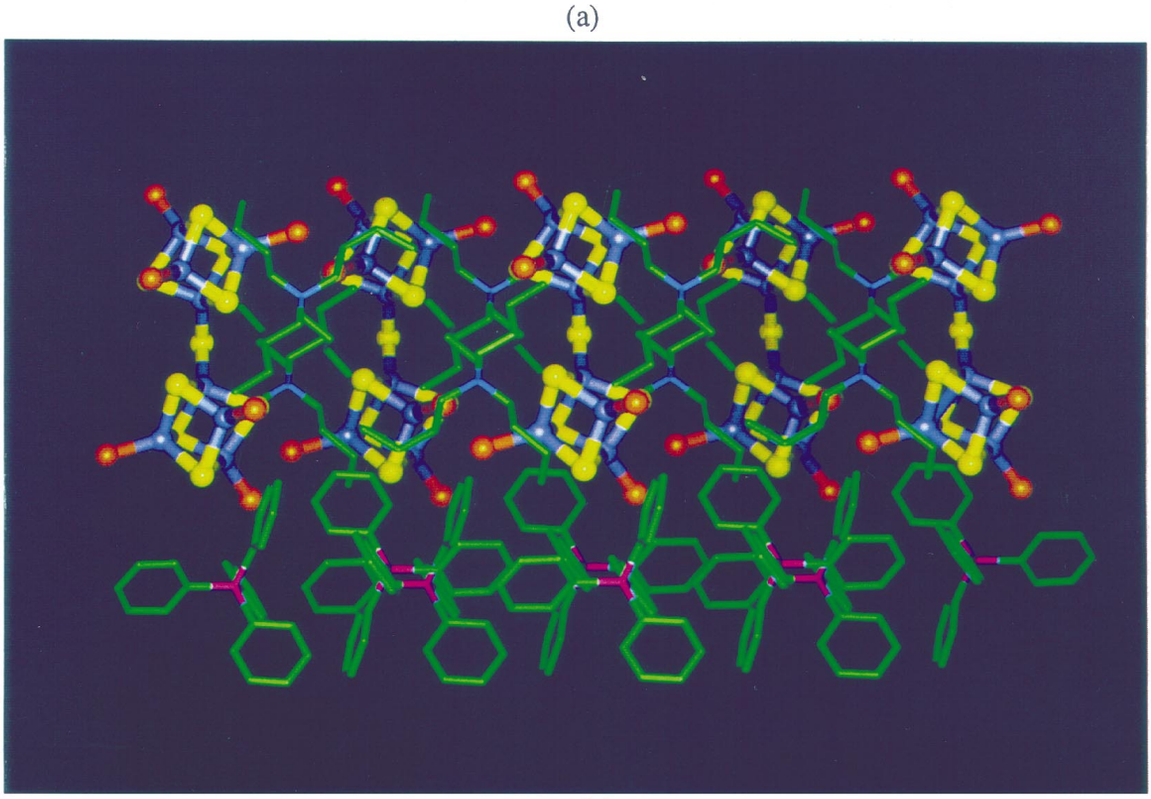

(b)

Fig. 2 Representations of the crystal structure of $[Ph_4P^+]_2[Bu_4N^+]_2[Fe_8S_9Cl_6]^{4-}$ [JEGBAY]. (a) View of the hexagonal ZZI6PE/P4PE layer of Ph_4P^+ cations, and the locations of the anions under the hexagons. (b) Side view of the layered structure, showing the segregated layer of Ph_4P^+ cations, with the Bu_4N^+ cations interspersed in the layer of anions.

$[Fe_4S_4(SH)_4]^{2-}$ [FAGREK] shown in Fig. 3. In both, the planes of the ZZI6PE sequences (as defined by the P atoms) are not exactly orthogonal, just as the C_{ipso}–P–C_{ipso} planes of the 4PE are not orthogonal (Table 2). However, the homologous compound $[Ph_4P^+]_2[Fe_4S_4I_4]^{2-}$ [KAKFIL] (Fig. 4) adopts the higher symmetry space group $I4_1/a$, crystallising with exact orthogonality between the directions of the ZZI6PE chains and between the normals to the P···P···P planes of the ZZI6PE chains. Within the O4PE, the two C_{ipso}–P–C_{ipso} planes are almost orthogonal. The P···P vector of the O4PE lies in the planes of both ZZI6PE chains. In this structure there is only one type of 6PE, one type of ZZI6PE, and one type of O4PE.

We have sought the reason for the subtle difference between $[Ph_4P^+]_2[Fe_4S_4Br_4]^{2-}$ [DEXXIN10] and $[Ph_4P^+]_2[Fe_4S_4I_4]^{2-}$

Table 2 Crystal structures containing two orthogonal ZZI6PE chains linked by a further 4PE

Refcode	Anion	P···P distances along ZZI6PE chain/Å	P···P distance in the 4PE/Å	Angle between normals to the two C_{ipso}–P–C_{ipso} planes of the 4PE/°
BECPII10[a]	$[NCCu(\mu\text{-}S)_2MoS_2]^{2-}$	6.45, 6.66	7.30	39.0
POPCEC[a]	$[NCCu(\mu\text{-}Se)_2MoSe_2]^{2-}$	6.46, 6.64	7.31	38.6
SUPZIM[a,b]	$[NCCu(\mu\text{-}Se)_2WSe_2]^{2-}$			
ZUPFIZ[a]	$[NCAu(\mu\text{-}Se)_2MoSe_2]^{2-}$	6.54, 6.62	7.25	39.2
FURHEF[a]	$[ClCo(N_3)_3]^{2-}$	6.44, 6.85	7.26	40.1
GEPFIQ[a]	$[MoSe_4]^{2-}$	6.47, 6.48	7.38	42.4
GEPFOW[a]	$[WSe_4]^{2-}$	6.47, 6.50	7.32	42.5
TADGAG[a]	$[NiCl_4]^{2-}$	6.37, 6.50	7.28	41.0
YUBDUU[a]	$[S_3NbSH]^{2-}$	6.42, 6.49	7.35	41.5
NAXXAL[a]	$[CdBr_4]^{2-}$	6.41, 6.65	7.41	32.9
DEXXIN10[c]	$[Fe_4S_4Br_4]^{2-}$	6.56, 6.69	7.37	67.6
FAGREK[c]	$[Fe_4S_4(SH)_4]^{2-}$	6.53, 6.69	7.48	66.9
KAKFIL	$[Fe_4S_4I_4]^{2-}$ space group $I4_1/a$	6.68	7.48	87.2
DAMNUA	$[Fe_4S_4Cl_2\{(\mu\text{-}S)_2CN(Et)_2\}_2]^{2-}$	6.54, 6.95	8.63	59.2

[a] These structures all have unit cells of similar dimensions, 11 × 20 × 20 Å, $\beta \approx 92°$. [b] No coordinates available, isostructural with POPCEC. [c] These two structures have unit cells of similar dimensions, 16 × 14 × 24 Å, $\beta \approx 110°$.

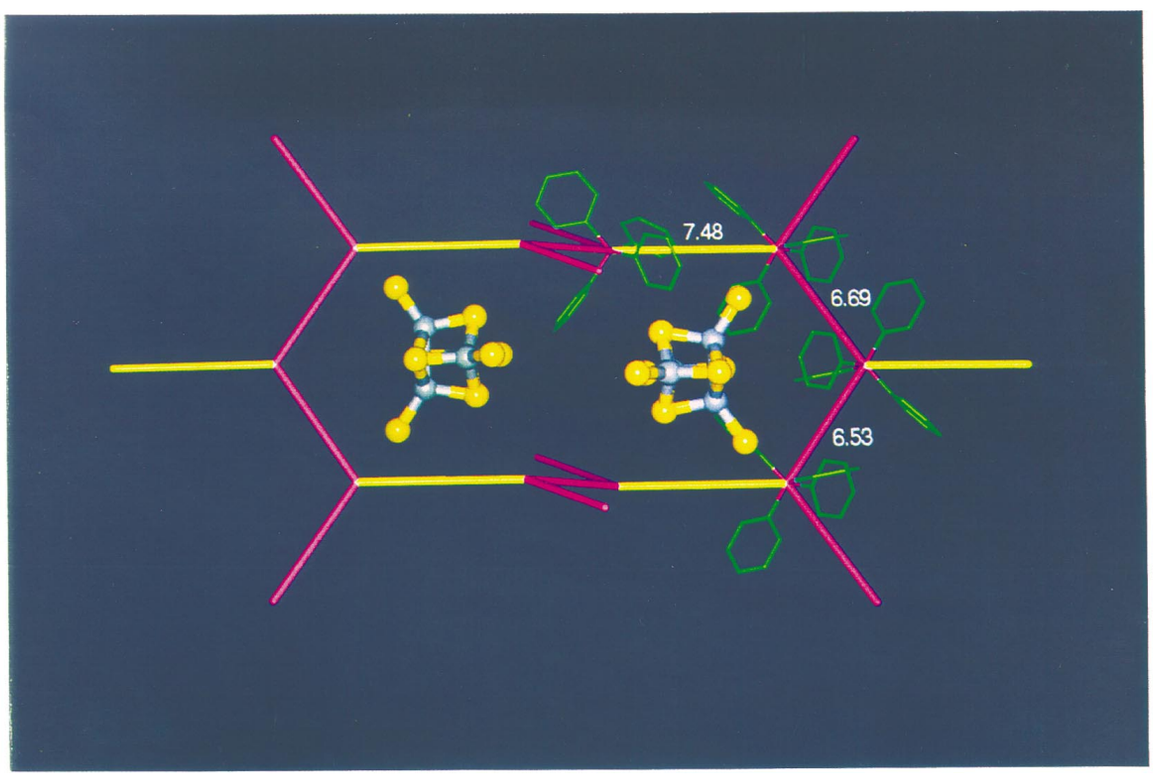

Fig. 3 Representation of the crystal structure of $[Ph_4P^+]_2[Fe_4S_4(SH)_4]^{2-}$ [FAGREK], with ZZI6PE chains denoted by the purple rods, and the O4PE motifs as yellow rods. One set of ZZI6PE chains runs top to bottom, the other almost perpendicular to the figure. An asymmetric set of phenyl groups is included, and the anion locations between the ZZI6PE chains are marked. The calculated energies of the embraces (identified by their P···P distances) are given in kcal mol^{-1} per $\{Ph_4\}_2$ set, and in square brackets per $\{Ph_4P\}_2$ set: 6PE at 6.53 Å, −9.1 [−6.1]; 6PE at 6.69 Å, −9.0 [−5.4]; O4PE at 7.48 Å, −5.9 [−2.8] kcal mol^{-1}.

[KAKFIL]. We believe that the network of embracing Ph_4P^+ around $[Fe_4S_4Br_4]^{2-}$ has distorted in order to contract the dimensions of the cavity containing the anion, and that the larger $[Fe_4S_4I_4]^{2-}$ anion has the correct volume for the ideal orthogonal ZZI6PE/O4PE network. The volumes of the anions in the three crystal lattices discussed here are $[Fe_4S_4(SH)_4]^{2-}$ [FAGREK] 231 $Å^3$, $[Fe_4S_4Br_4]^{2-}$ [DEXXIN10] 238 $Å^3$, and $[Fe_4S_4I_4]^{2-}$ [KAKFIL] 264 $Å^3$, supporting this view.

Corrugated sheets with eight-rings of Ph_4P^+

The compound $[Ph_4P^+]_3[CRe_7(CO)_{21}]^{3-}$ [BEJBOH] crystallises with a two-dimensional network of cations engaged in different types of multiple phenyl embraces. The essential features of the crystal packing are shown in Fig. 5. The cation array is comprised of centrosymmetric sequences of five 6PE, linked by P4PE (P···P 8.43 Å) and 4PE (P···P 7.23 Å) interactions into eight-membered cycles, and the anions lie over these eight-rings. Note that the larger eight-ring here, relative to the six-rings in the pseudo-hexagonal cation arrays already described, accommodates the larger size of the anion and its 3− charge: the stoichiometry of cation contributions in an eight-ring is $(6 \times \frac{1}{3}) + (2 \times \frac{1}{2}) = 3+$. The sheets of cations are corrugated (see Fig. 5) and the anions nestle in the hollows.

More elaborate three-dimensional networks of Ph_4P^+

Fig. 6 represents the crystal lattice of $[Ph_4P^+]_2[Te_4]^{2-}$ [KIZWEV] which contains two different well-developed zig-zag chains of SPE, both running in the same direction, and linked in the

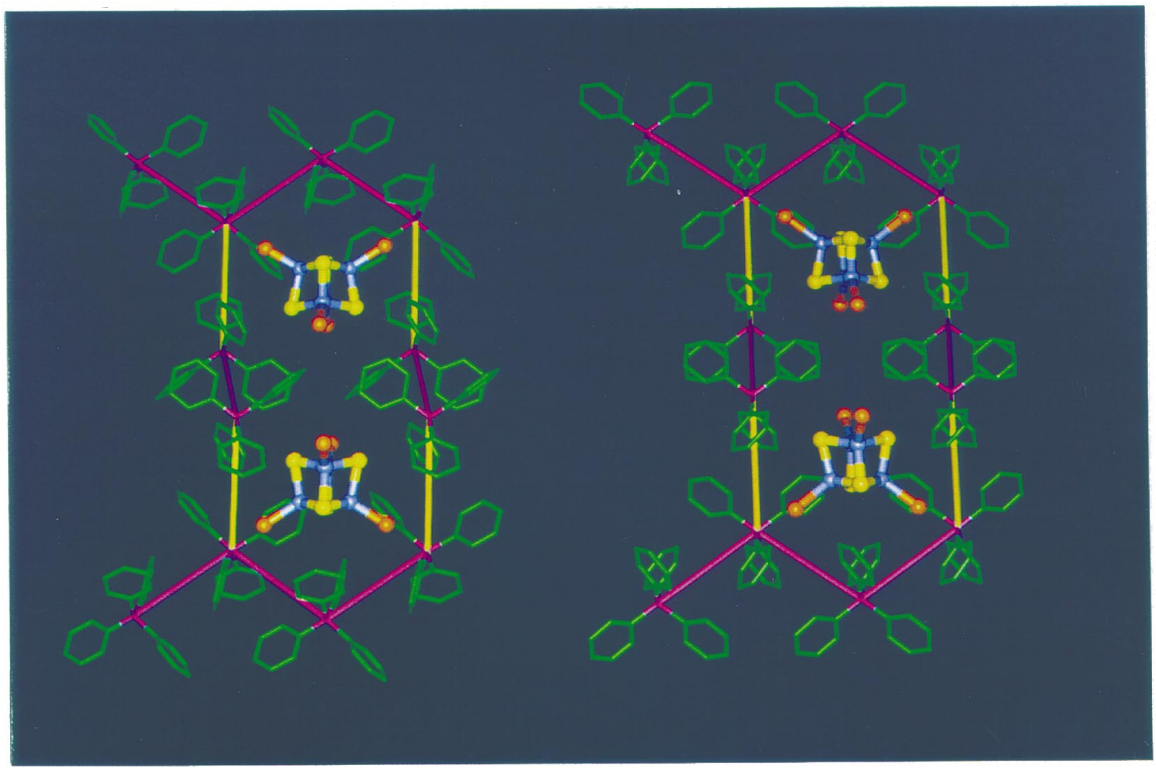

Fig. 4 Comparison of the crystal structures of $[Ph_4P^+]_2[Fe_4S_4Br_4]^{2-}$ [DEXXIN10] in space group $C2/c$ (left) and $[Ph_4P^+]_2[Fe_4S_4I_4]^{2-}$ [KAKFIL] in space group $I4_1/a$ (right). Colour coding is as for Fig. 3. The slight distortions of the lattice in DEXXIN10 are obvious. Only one 6PE of the ZZI6PE chain parallel to the viewing direction can be seen.

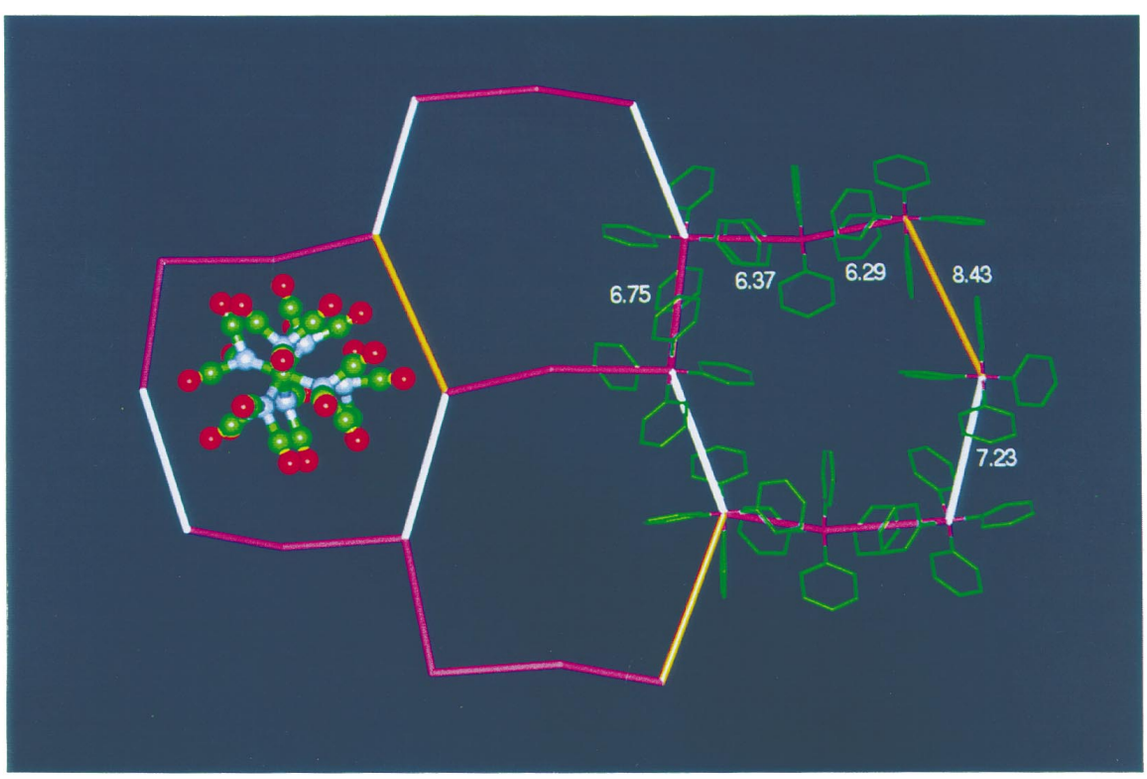

Fig. 5 Simplification of the crystal structure of $[Ph_4P^+]_3[CRe_7(CO)_{21}]^{3-}$ [BEJBOH]. Purple rods signify 6PE, orange rods are P4PE, and the white rods are asymmetric 4PE. This view of the P4PE at 8.43 Å illustrates well the offset-face-to-face and two edge-to-face Ph···Ph interactions characteristic of P4PE. Note that the cation involved in the 6PE identified as 6.37, 6.29 Å is folded out of the cation layer, and that this occurs in such a way that the sheet of cations is corrugated left-right across the figure. The calculated energies of the embraces (identified by their P···P distances) are given in kcal mol^{-1} per $\{Ph_4\}_2$ set, and in square brackets per $\{Ph_4P\}_2$ set: 6PE at 6.29 Å, −8.9 [−5.9]; 6PE at 6.37 Å, −6.7 [−3.3]; 6PE at 6.75 Å, −4.8 [−1.9]; 4PE at 7.23 Å, −5.2 [−2.6]; P4PE at 8.43 Å, −4.1 [−1.0] kcal mol^{-1}.

other two dimensions. One set of ZZI6PE (P···P 5.98, 6.34 Å) is linked by P4PE to form the hexagonal ZZI6PE/P4PE layer already described, while the other set of ZZI6PE (P···P 6.39, 6.72 Å) does not contain these links. The two sets of ZZI6PE alternate through the crystal lattice, and are linked by 3PE in which a phenyl ring on one cation is directed between the pair

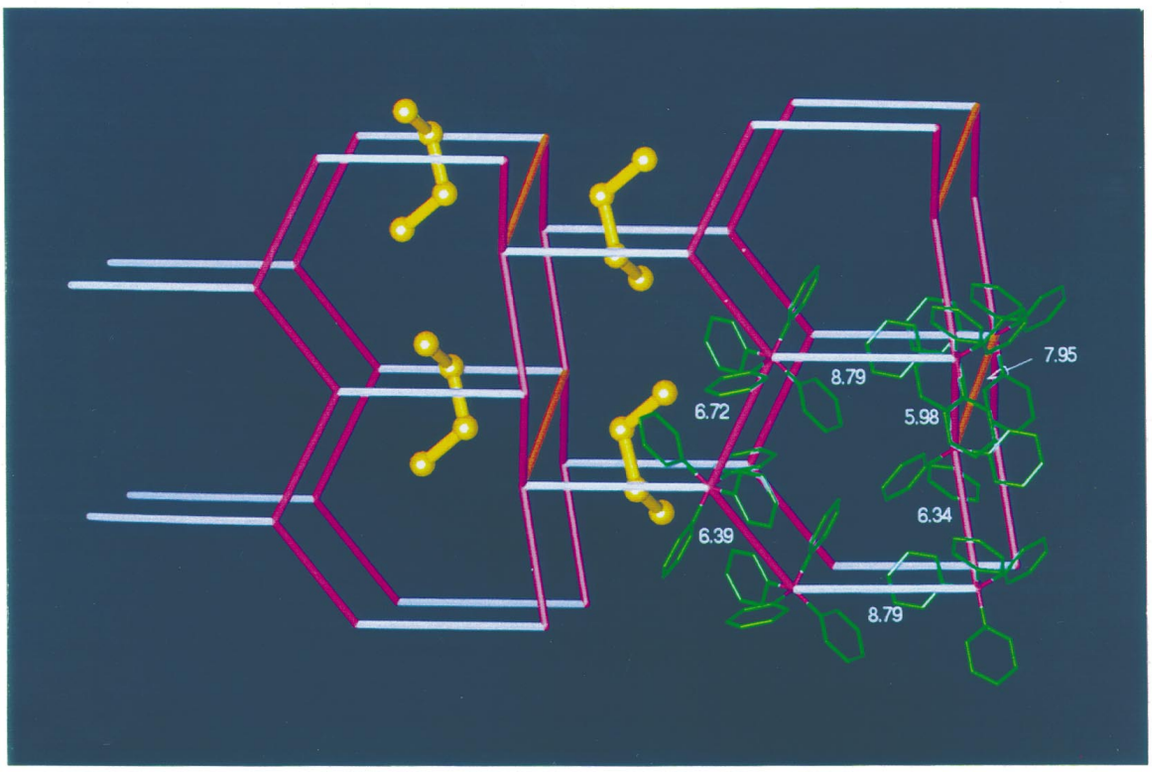

Fig. 6 Representation of the labyrinth of multiple phenyl embraces in crystalline $[Ph_4P^+]_2[Te_4]^{2-}$ [KIZWEV]. The purple rods signify 6PE, orange P4PE, and grey 3PE (P···P 7.95 Å) in which one phenyl ring of one cation is attracted to two phenyl rings on the adjacent cation. The calculated energies of the embraces (identified by their P···P distances) are given in kcal mol^{-1} per $\{Ph_4\}_2$ set, and in square brackets per $\{Ph_4P\}_2$ set: 6PE at 5.98 Å, −10.4 [−7.2]; 6PE at 6.34 Å, −9.9 [−6.2]; 6PE at 6.39 Å, −9.2 [−6.1]; 6PE at 6.72 Å, −7.6 [−4.4]; P4PE at 7.95 Å, −5.8 [−2.6]; 3PE at 8.79 Å, −4.7 [−1.9] kcal mol^{-1}.

of phenyl rings external to an adjacent ZZI6PE and forms attractive edge-to-face interactions with them. As shown in Fig. 6 the abnormally small anions thread between these 3PE. The majority of the crystal lattice is comprised of Ph_4P^+ cations in attractive embraces.

An even more elaborate network of multiple phenyl embraces occurs in $[Ph_4P^+]_4[(S_6)Cu(S_8)Cu(S_6)]^{4-}$ [COVCAR], shown in Fig. 7. ZZI6PE chains are a prominent feature, and they occur as two types, one (type A) with P···P separations of 6.29, 6.90 Å, the other (type B) 6.27, 6.97 Å. ZZI6PE chains of each type occur in layers, and form pseudo-hexagonal planar networks, although the connections (P···P 8.75, 8.65 Å respectively) between the chains in each network are long and not significant. The layers are viewed almost edge-on in Fig. 7. Between the planar hexagonal layers (A, B) of cations there are puckered hexagonal nets of cations (type C), connected by 6PE and P4PE as fused six-rings in chair conformation. Cations in the planar layers and the puckered layers are further connected by 3PE (P···P 8.55 Å for A to C and P···P 8.39 Å for B to C). The sequence of layers of cations, evident in Fig. 7, is then –A–(3PE)–C–(3PE)–B–(3PE)–C–(3PE)–A–. Cations in the puckered layers (C) are four-connected, while cations in planar layers (A,B) are effectively three-connected because the 8.65, 8.75 Å linkages are insignificant. The very flexible anion, in extended conformation, threads through this labyrinth of cations: each CuS_6 chelate unit in the anion is located between a planar layer and a puckered layer of cations, in a pseudo-adamantanoid cage of cations. Our interpretation of the crystal packing in this compound is that the aggregate of the attractive energies of the embracing cations will be the dominant contribution to the lattice energy, and that intramolecular energies for the anion will have negligible effect. The calculated energies of the identified motifs are included in the caption to Fig. 7.

We note that the network of alternating planar and puckered layers of six-rings, *i.e.* alternating graphitic and diamondoid layers, which occurs in $[Ph_4P^+]_4[(S_6)Cu(S_8)Cu(S_6)]^{4-}$ is present also in the crystal structure of a quite different copper sulfide compound, the CuS mineral covellite.[14]

Lastly, we describe briefly a crystal structure which manifests a one-dimensional chain containing 6PEs which is different from the ZZI6PE motif. In $Ph_4P^+[CpMo(Se_4)_2]^-$ [SIRGAB] there is a ladder motif which is dominated by repeated 6PEs, but as illustrated in Fig. 8(a) there are other appreciable Ph···Ph attractive energies within the ladder. Fig. 8(b) shows the separation of these layers by the $[CpMo(Se_4)_2]^-$ anions.

Discussion

We have shown that sequences of 6PE, particularly as the ZZI6PE, are prevalent in crystals containing Ph_4P^+, and that they further associate through well developed multiple phenyl embraces to form two-dimensional and three-dimensional networks of Ph_4P^+. The combination of the ZZI6PE and the P4PE is the most common structure type, forming two-dimensional nets of cations arranged in hexagons which are skewed as a requirement of the P4PE. Alternatively, orthogonal ZZI6PE chains can be linked through O4PE.

There is substantial chemical diversity in the anions which form these networks, particularly the ZZI6PE/P4PE net, although there is a preponderance of doubly negative anions and of anions containing chalcogenide and polychalcogenide metal complexes. This latter bias reflects laboratory custom, and the knowledge of preparative chemists exploring these areas that the Ph_4P^+ cation generates good crystals of such anions. We predict that more widespread use of Ph_4P^+ as a crystallising cation will broaden the scope of the crystals demonstrating the networks of multiple phenyl embraces described here.

We note that the majority of the crystals described in the preceding paper,[7] with networks based on the 4PE, contain mono-negative anions, while the majority of crystals forming more elaborate networks of 6PE (this paper) contain di-

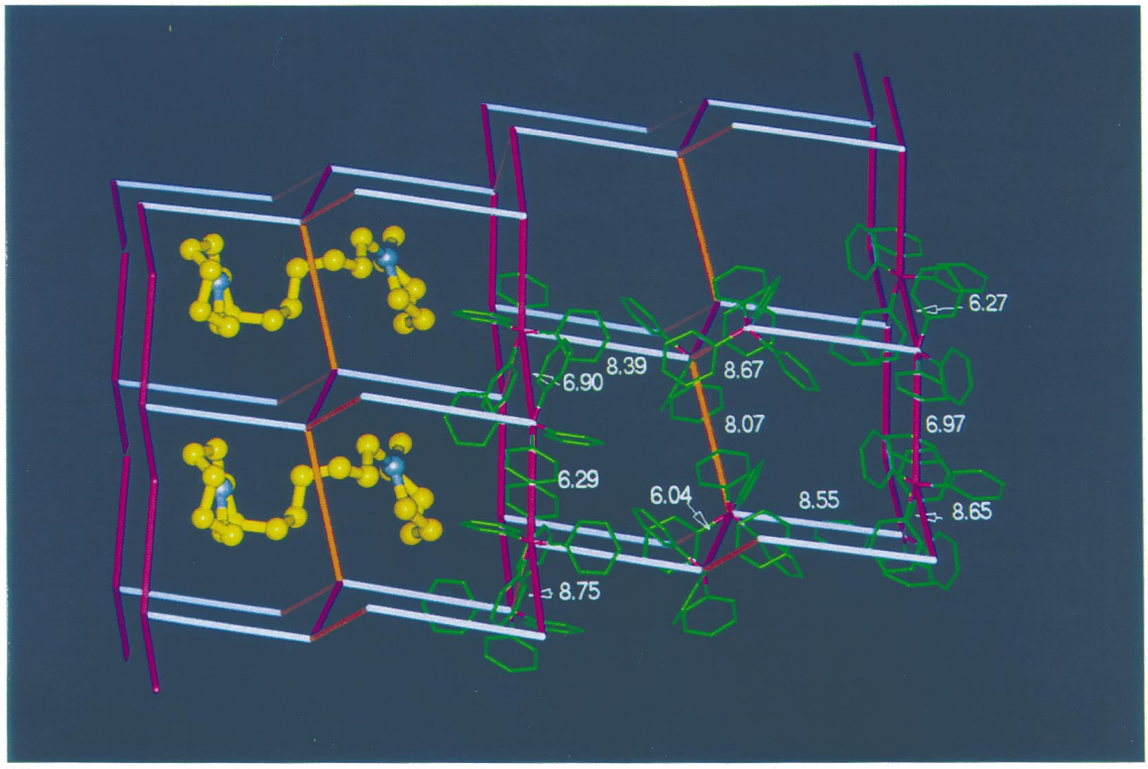

Fig. 7 Representation of part of the crystal packing and multiple phenyl embraces in $[Ph_4P^+]_4[(S_6)Cu(S_8)Cu(S_6)]^{4-}$ [COVCAR]. Purple rods signify 6PE, orange rods are P4PE, and grey rods are 3PE. The anion has CuS_6 chelate rings linked by an extended S_8 chain. The calculated energies of the embraces (identified by their P···P distances) are given in kcal mol^{-1} per $\{Ph_4\}_2$ set, and in square brackets per $\{Ph_4P\}_2$ set: 6PE at 6.04 Å, −10.2 [−7.4]; 6PE at 6.27 Å, −8.5 [−5.4]; 6PE at 6.29 Å, −7.4 [−4.7]; 6PE at 6.90 Å, −8.5 [−5.2]; 6PE at 6.97 Å, −6.8 [−3.1]; P4PE at 8.07 Å, −5.2 [−2.4]; 3PE at 8.39 Å, −0.5 [+2.1]; 3PE at 8.55 Å, −4.4 [−1.4]; 4PE at 8.67 Å, −2.7 [+0.3] kcal mol^{-1}.

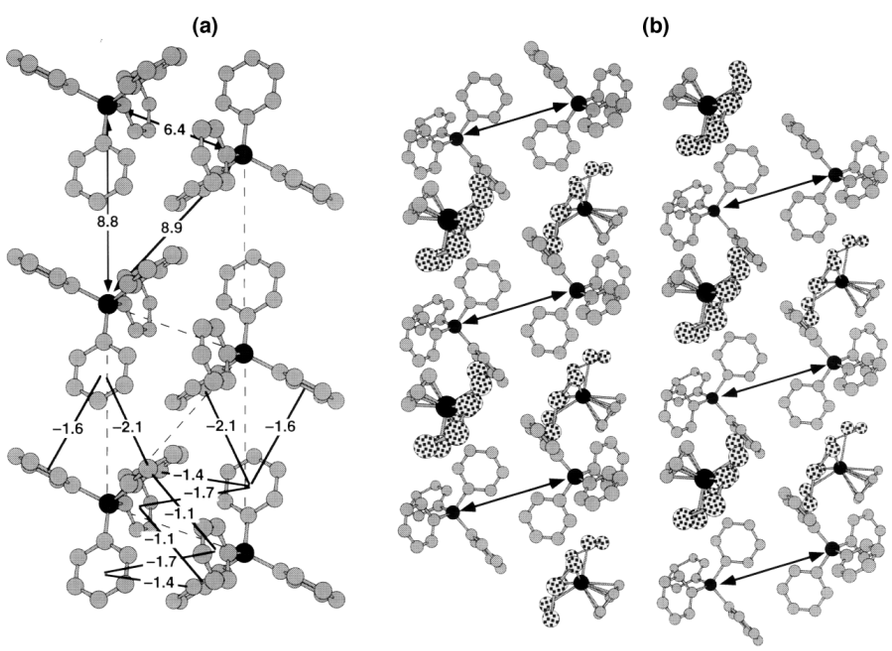

Fig. 8 Representations of the crystal packing in $Ph_4P^+[CpMo(Se_4)_2]^-$ [SIRGAB]: P, Mo black, C grey, Se speckled, H atoms omitted for clarity. (a) Face view of the ladder: P···P distances are marked with arrows, while the non-arrowed numbers are the energies (kcal mol^{-1} per Ph_2) between individual phenyl rings. The centrosymmetric 6PE (6.4 Å) and the strong attractive interactions along the edges of the ladder are evident. (b) View along the ladders (marked with arrows) showing how the ladders are separated by the $[CpMo(Se_4)_2]^-$ anions.

negative anions. What is the reason for this pattern? The 4PE layer has one positive charge per cycle and so can conveniently accommodate one X^- anion above (or below) each cycle. The 6PE layer has two positive charges per cycle and so can accommodate one X^{2-} anion per cycle. Alternatively, there can be one X^- on each side of the cycle, and this has been found to occur. Because of the relatively large space between layers, solvent is often accommodated there also.

A crystal structure which might be expected is the one-dimensional motif comprised of an isolated pair of ZZI6PE linked by P4PE to form a ladder (analogous to those in the preceding paper): this would be a one-dimensional section of

Table 3 Total calculated attractive energies between one Ph_4P^+ cation and neighbouring Ph_4P^+ cations in crystals containing networks of 6PE and other multiple phenyl embraces

Crystal refcode	Number of surrounding Ph_4P^+ cations	Types of multiple phenyl embraces	Total interaction energy per Ph_4P^+ [a]/kcal mol^{-1}
VIPTAP	3	$(6PE)_2(P4PE)$	−7.0
			−5.1
FAGREK	3	$(6PE)_2(O4PE)$	−7.2
BEJBOH	2	$(6PE)_2$	−4.6
BEJBOH	3	$(6PE)_2(4PE)$	−3.9
BEJBOH	3	(6PE)(4PE)(P4PE)	−4.8
KIZWEV	3	$(6PE)_2(3PE)$	−6.2
KIZWEV	4	$(6PE)_2(P4PE)(3PE)$	−8.9
COVCAR	4	$(6PE)_2(P4PE)(3PE)$	−4.0
COVCAR	4	(6PE)(P4PE)(3PE)(4PE)	−5.5
			−3.7
COVCAR	4	$(6PE)_2(4PE)(3PE)$	−4.5
VOFMOS	3	$(6PE)_2(P4PE)$	−8.5
			−7.9

[a] Intermolecular energy contributions from all atoms in Ph_4P^+ are included. The energy is per Ph_4P^+: each local intermolecular interaction energy is halved before the summation, so that no energies are doubly counted.

the two-dimensional ZZI6PE/P4PE net. However we have not yet found an instance of this: the closest approach to this type is SIRGAB, Fig. 8.

The networks described in this paper raise the question about the number of multiple phenyl embraces which can be sustained by a Ph_4P^+ cation, and the total attractive energy involved. The most common pattern is $(6PE)_2(4PE)$ at one Ph_4P^+, and for this we calculate that each 6PE contributes *ca.* 7 kcal mol^{-1} of attractive energy per $[Ph_4P^+]_2$ pair and the 4PE *ca.* 3 kcal mol^{-1} of attractive energy per $[Ph_4P^+]_2$ pair (in the following discussion the contributions from all atoms of the Ph_4P^+ cations are included in the energies quoted). Two of the structures illustrated show one Ph_4P^+ cation participating in four multiple phenyl embraces: in KIZWEV (Fig. 6) there are are two 6PE, one P4PE, and one 3PE linking to one cation, while in COVCAR (Fig. 7) different Ph_4P^+ cations participate in one 6PE, two 4PE and one 3PE, or two 6PE, one 4PE and one 3PE.

Of greater significance to the crystal packing energy is the total interaction energy between a cation and its neighbouring cations, not subdivided according to type or number of local motifs. For this we calculate the energies given in Table 3. It appears that the maximum attractive interaction energy which a Ph_4P^+ can achieve with surrounding Ph_4P^+ cations participating in multiple phenyl embraces is *ca.* 9 kcal mol^{-1}.

All of these embraces between Ph_4P^+ cations are as strong as conventional hydrogen bonds, and the extended supramolecular motifs demonstrated here are dominant lattice-determining factors.

Acknowledgements

This research is funded by the Australian Research Council through a project grant and through VisLab computing facilities.

References

1 I. G. Dance and M. L. Scudder, *J. Chem. Soc.*, *Chem. Commun.*, 1995, 1039.
2 I. G. Dance, in *The Crystal as a Supramolecular Entity*, ed. G. R. Desiraju, John Wiley, New York, 1996, pp. 137–233.
3 I. Dance and M. Scudder, *Chem. Eur. J.*, 1996, **2**, 481.
4 C. Hasselgren, P. A. W. Dean, M. L. Scudder, D. C. Craig and I. G. Dance, *J. Chem. Soc.*, *Dalton Trans.*, 1997, 2019.
5 I. Dance and M. Scudder, *New J. Chem.*, 1998, 481.
6 M. Scudder and I. Dance, *J. Chem. Soc.*, *Dalton Trans.*, 1998, 329.
7 M. Scudder and I. Dance, preceding paper.
8 J. D. Dunitz, *Pure Appl. Chem.*, 1991, **63**, 177.
9 G. R. Desiraju, *The Crystal as a Supramolecular Entity*, *Perspectives in Supramolecular Chemistry*, ed. J. M. Lehn, John Wiley, Chichester, 1996.
10 F. H. Allen and O. Kennard, *Chem. Des. Automat. News*, 1993, **8**, 131.
11 I. Dance and M. Scudder, *J. Chem. Soc.*, *Dalton Trans.*, 1996, 3755.
12 N. A. Ahmed, A. I. Kitaigorodsky and K. V. Mirskaya, *Acta Crystallogr. Sect. B*, 1971, **27**, 867.
13 C. P. Brock and J. D. Dunitz, *Chem. Mater.*, 1994, **6**, 1118.
14 H. J. Gotsis, A. C. Barnes and P. Strange, *J. Phys. Condens. Matter*, 1992, **4**, 10461.

Paper 8/03464H